BTBR *Ob/Ob* Mutant Mice Model Progressive Diabetic Nephropathy

Kelly L. Hudkins,* Warangkana Pichaiwong,* Tomasz Wietecha,* Jolanta Kowalewska,* Miriam C. Banas,*† Min W. Spencer,* Anja Mühlfeld,*‡ Mariko Koelling,* Jeffrey W. Pippin,§ Stuart J. Shankland,§ Bardia Askari,* Mary E. Rabaglia,‖ Mark P. Keller,‖ Alan D. Attie,‖ and Charles E. Alpers*§

*Department of Pathology and §Division of Nephrology, Department of Medicine, University of Washington, Seattle, Washington; †Division of Nephrology, University of Regensburg, Regensburg, Germany; ‡Division of Nephrology, University of Aachen, Aachen, Germany; and ‖Department of Biochemistry, University of Wisconsin, Madison, Wisconsin

ABSTRACT

There remains a need for robust mouse models of diabetic nephropathy (DN) that mimic key features of advanced human DN. The recently developed mouse strain BTBR with the *ob/ob* leptin-deficiency mutation develops severe type 2 diabetes, hypercholesterolemia, elevated triglycerides, and insulin resistance, but the renal phenotype has not been characterized. Here, we show that these obese, diabetic mice rapidly develop morphologic renal lesions characteristic of both early and advanced human DN. BTBR *ob/ob* mice developed progressive proteinuria beginning at 4 weeks. Glomerular hypertrophy and accumulation of mesangial matrix, characteristic of early DN, were present by 8 weeks, and glomerular lesions similar to those of advanced human DN were present by 20 weeks. By 22 weeks, we observed an approximately 20% increase in basement membrane thickness and a >50% increase in mesangial matrix. Diffuse mesangial sclerosis (focally approaching nodular glomerulosclerosis), focal arteriolar hyalinosis, mesangiolysis, and focal mild interstitial fibrosis were present. Loss of podocytes was present early and persisted. In summary, BTBR *ob/ob* mice develop a constellation of abnormalities that closely resemble advanced human DN more rapidly than most other murine models, making this strain particularly attractive for testing therapeutic interventions.

J Am Soc Nephrol 21: 1533–1542, 2010. doi: 10.1681/ASN.2009121290

Diabetic nephropathy (DN) is the largest single cause of ESRD in the United States, accounting for nearly half of the patients who enter the dialysis patient population each year and currently accounting for 45% of prevalent kidney failure in the United States.[1–4] Although both type 1 and type 2 diabetes lead to DN, the current epidemic of DN is due to type 2 diabetes; however, understanding the mechanisms that produce the constellation of clinical and pathologic alterations that define DN in humans remains very incomplete, in part because clinical DN is a slowly progressive disease, and relevant animal models that produce this constellation of pathologic and clinical abnormalities have important limitations. Mice rendered hyperglycemic by administration of streptozotocin (STZ) or through genetic predisposition such as the *db/db* mouse can develop some features of DN, most notably glomerular mesangial expansion, but do so only over prolonged periods and do not progress to ESRD.[5–9] Most murine models to date have failed to develop reliably marked mesangial expansion or the

Received December 23, 2009. Accepted May 16, 2010.

Published online ahead of print. Publication date available at www.jasn.org.

Correspondence: Dr. Charles E. Alpers, University of Washington Medical Center, Department of Pathology, Box 356100, 1959 NE Pacific Street, Seattle, WA 98195. Phone: 206-598-6409; Fax: 206-543-3644; E-mail: calp@u.washington.edu

distinctive nodular glomerulosclerosis with mesangiolysis or hyalinosis characteristic of human disease. Furthermore, the extent of loss or preservation of podocytes, currently accepted to be important in human DN, is generally unknown in each of these models.[10] Thus, the availability of a murine model of DN that better resembles its human counterpart and in particular develops glomerular lesions of podocyte loss, mesangiolysis, and severe sclerosis would be a new and significant resource for mechanistic investigations of DN and to test potential therapeutic interventions.

A mouse model of insulin resistance that develops in the progeny of the BTBR (black and tan, brachyuric) mouse strain crossed with C57BL/6 mice has been characterized by Attie and colleagues.[11,12] BTBR mice are naturally hyperinsulinemic when compared with C57BL/6 mice, and BTBR × C57BL/6 F1 mice are substantially insulin resistant.[11,12] Mice homozygous for the *ob/ob* mutation lack the hormone leptin. When this mutation is on the C57BL/6 background, mice become obese but are only mildly hyperglycemic and do not develop renal lesions characteristic of human diabetes. When the *ob/ob* mutation is placed on a BTBR background, the mice are initially insulin resistant with elevated insulin levels and pancreatic islet hypertrophy and have marked hyperglycemia by 6 weeks of age.[11–15] The C57BL/6 and BTBR strains, when made obese by introduction of the *ob/ob* mutation, differ significantly in their diabetes susceptibility; C57BL/6 *ob/ob* mice are insulin resistant but relatively diabetes resistant, whereas BTBR *ob/ob* mice are insulin resistant and develop severe diabetes.[13] BTBR *ob/ob* mice maintain sustained hyperglycemia (blood glucose 350 to 400 mg/dl) and are largely resistant to the blood glucose–lowering effect of insulin administration. Although there are some sex differences in the diabetic disease manifestations, particularly in the early course of the disease, both sexes are ultimately affected by severe diabetes. In this study, we characterize the development of DN in both the male and female BTBR *ob/ob* mice.

RESULTS

Blood and Urine Parameters

Both male and female BTBR *ob/ob* mice have significantly increased blood glucose levels and body weight detectable at 8 weeks when compared with heterozygous BTBR $ob^{+/-}$ and BTBR wild-type (WT) littermates (Table 1, Supplemental Figure 1). Male mice progressed to somewhat higher blood glucose levels, averaging 399.0 ± 38.8 mg/dl at 22 weeks compared with female mice with an average of 333.0 ± 46.3 mg/dl (Table 1). Compared with obese C57BL/6 *ob/ob* mice, BTBR *ob/ob* mice have significantly higher blood glucose levels (Table 1). Despite the early hyperglycemia, the growth rate of BTBR *ob/ob* mice was similar to that of nondiabetic C57BL/6 *ob/ob* mice (data not shown). Serum triglyceride, cholesterol, and blood urea nitrogen (BUN) levels were elevated in both male and female

Table 1. Representative laboratory data for BTBR *ob/ob* mice and C57BL/6 control mice all between 20 and 22 weeks of age ($n = 6$)

Parameter	Female			
	C57BL/6	C57BL/6 *ob/ob*	BTBR	BTBR *ob/ob*
Glucose (mg/dl)	135.0 ± 7.5	159.5 ± 7.2	133 ± 10.2	333 ± 46.3[a,b]
BUN (mg/dl)	35.8 ± 8.0	26 ± 2.9	27.9 ± 3.0	29.0 ± 7.0
Creatinine (HPLC; mg/dl)	ND	ND	0.211 ± 0.024	0.256 ± 0.069
Cholesterol (mg/dl)	53.5 ± 6.4	95.8 ± 8.2[c]	93.8 ± 5.5[b]	151.5 ± 26.9[a,b]
Triglycerides (mg/dl)	47.5 ± 2.5	65.0 ± 5.0	50.8 ± 4.8	96.3 ± 31.8[c]
HDL (mg/dl)	34.5 ± 5.6	63.8 ± 8.8[a]	64.9 ± 4.4[b]	79 ± 10.5[b]
ACR (μg/mg)	26.2 ± 6.9	195.9 ± 29.1	94.1 ± 18.9[b]	969.9 ± 139.9[a,b]
Albumin, 24-hour (μg)	9.1 ± 3.7	54.0 ± 20.0	21.32 ± 7.8	248.7 ± 47.1[a,d]
	Male			
	C57BL/6	C57BL/6 *ob/ob*	BTBR	BTBR *ob/ob*
Glucose (mg/dl)	159.5 ± 10.5	245.4 ± 33.7[a]	147 ± 16.4	399 ± 38.8[a,b]
BUN (mg/dl)	34.8 ± 4.5	36.7 ± 2.1	19.5 ± 5.0[b]	35.0 ± 11.3[a]
Creatinine (HPLC; mg/dl)	ND	ND	0.180 ± 0.030	0.148 ± 0.024
Cholesterol (mg/dl)	57 ± 5.5	165.2 ± 14.6[a]	115.2 ± 7.5[b]	194.3 ± 21.9[a,e]
Triglycerides (mg/dl)	49.3 ± 6.9	103 ± 2.7[c]	129.8 ± 40[b]	196.1 ± 34.2[a,b]
HDL (mg/dl)	33.8 ± 5.2	112.8 ± 9.3[a]	83.5 ± 14.2[b]	88.5 ± 13.9[b]
ACR (μg/mg)	46.9 ± 7.1	263.5 ± 67.7[c]	51.1 ± 11.7	809.5 ± 134.1[a,b]
Albumin, 24-hour (μg)	13.6 ± 3.3	111.6 ± 36.5	17.2 ± 6.0	241.8 ± 45.2[a,d]

Controls include C57BL/6 mice with and without the *ob/ob* mutation. ACR, albumin-creatinine ratio; ND, not done (sera from the 20- to 22-week-old C57BL/6 and C57BL/6 *ob/ob* mice had been exhausted).
[a] $P < 0.001$ *versus* WT of same gender and background strain.
[b] $P < 0.001$ *versus* C57BL/6 of same gender and *ob* mutation status.
[c] $P < 0.01$ *versus* WT of same gender and background strain.
[d] $P < 0.01$ *versus* C57BL/6 of same gender and *ob* mutation status.
[e] $P < 0.05$ *versus* C57BL/6 of same gender and *ob* mutation status.

BTBR *ob/ob* mice compared with WT littermates, although serum creatinine levels measured by both colorimetric and HPLC methods were not significantly different (Table 1).

The BTBR *ob/ob* mice developed albuminuria, with increased albumin-creatinine ratios measured in spot urine samples (Table 1, Figure 1). Elevated albuminuria was detectable as early as 8 weeks of age (Figure 1) and remained elevated thereafter, achieving a 10-fold difference by age 20 weeks. When timed urine collections were obtained, there was also a >10-fold increase in albumin excretion in both male and female BTBR *ob/ob* mice when compared with littermate controls at 20 weeks (Table 1). Mice were studied up to the age of 22 to 24 weeks, because around this age and beyond, there was greatly increased mortality for reasons yet to be identified.

Renal Structural Alterations

Obese, diabetic BTBR *ob/ob* mice exhibited renal hypertrophy compared with their BTBR WT littermates (Supplemental Table 1). Compared with C57BL/6 *ob/ob* mice, which were similarly obese, BTBR *ob/ob* mice had increased kidney weight, as did BTBR WT mice compared with C57BL/6 WT mice (Supplemental Table 1).

BTBR *ob/ob* mice develop renal lesions that consist of increasing glomerular mesangial matrix accumulation and are detectable histologically as early as 8 weeks of age (Figure 2). This mesangial matrix accumulation is either preceded or accompanied by episodes of mesangiolysis, because mesangiolysis can be detected in approximately 8% of glomeruli in tissue sections obtained from 8-week-old BTBR *ob/ob* mice (Figure 3, A and B). The degree of mesangiolysis increases with age, reaching an average of 24.5% of glomeruli exhibiting mesangiolysis at 16 weeks and 33.1% at 22 weeks of age in female mice (Figures 2K and 3, B through D). Male BTBR *ob/ob* mice had qualitatively similar degrees of mesangiolysis. In contrast, C57BL/6 *ob/ob* mice do not have markedly increased mesangial matrix or mesangiolysis (Figure 3E). Morphologically advanced glomerular abnormalities identified in both male and female BTBR *ob/ob* mice include diffuse and, rarely, nodular mesangial sclerosis (Figures 2, F and H, and 4), mesangiolysis (Figures 2K and 3, B through D), focal and mild interstitial fibrosis (Supplemental Figure 2), and, very focally, arteriolar hyalinosis (Figure 2H). Computer-aided morphometry, performed on collagen IV–immunostained tissue sections demonstrated significantly increased glomerular size and progressive accumulation of matrix in both male and female BTBR *ob/ob* mouse (Table 2, Supplemental Figure 3).

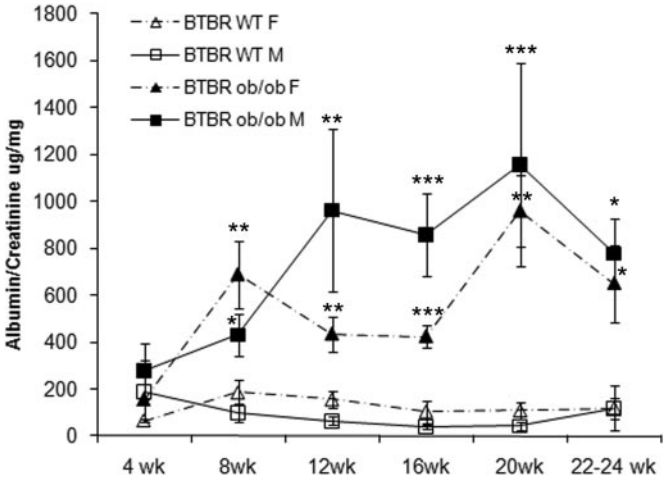

Figure 1. BTBR *ob/ob* mice have markedly increased albuminuria. Albumin-creatinine ratios are significantly increased in BTBR *ob/ob* mice beginning at 8 weeks of age and remain elevated thereafter. There is a peak difference at 20 weeks, which becomes less marked at later time points as a result of increased mortality of the most severely affected mice, which can no longer be included in these measurements. ***$P < 0.001$, **$P < 0.01$, *$P < 0.05$ *versus* age- and gender-matched BTBR WT mice.

Measurement of glomerular capillary basement membrane thickness by electron microscopy showed an increase of 18% in BTBR *ob/ob* relative to BTBR WT at 20 weeks (181.4 ± 3.8 *versus* 152.9 ± 5.1 nm; $n = 7$; $P < 0.001$). Both electron microscopy and immunofluorescence confirmed the absence of immune deposits (Figure 4, Supplemental Figure 4).

Immunostaining for α-smooth muscle actin (α-SMA), a marker of mesangial cell activation, and for Mac-2–positive monocyte/macrophages revealed that both were increased significantly in BTBR *ob/ob* mice compared with WT littermate controls. Increased Mac-2–positive cells were first detected in the glomerular capillaries of 12-week-old BTBR *ob/ob* mice, later than when both podocyte loss and mesangiolysis were first detected, and after changes of marked mesangial matrix expansion were already present (Table 3). Measurement of actin-positive mesangial cells within glomeruli was significantly increased in both male and female BTBR *ob/ob* mice at 22 weeks compared with WT littermates (3.70 ± 0.70 *versus* 0.17 ± 0.05% [$P < 0.001$] and 1.49 ± 0.46 *versus* 0.20 ± 0.06% [$P < 0.05$], respectively).

Importantly, BTBR *ob/ob* mice do not develop atherosclerosis (data not shown), and they do not develop hypertension. In fact, BTBR *ob/ob* mice are hypotensive compared with BTBR WT and heterozygous controls (Supplemental Figure 5), likely a direct consequence of leptin deficiency.[16,17]

Podocyte Number and Density

Podocyte number and density were measured at two time points, 8 and 20 weeks in BTBR WT and BTBR *ob/ob* mice and at 24 ($n = 6$) and 28 ($n = 7$) weeks in BTBR *ob/ob* mice only (Table 4). Podocyte number was reduced to an equivalent degree in BTBR *ob/ob* mice using both the Weibel and Sanden methods. Podocyte density was significantly reduced in BTBR *ob/ob* mice compared with BTBR WT mice at every time point studied (data using Sanden method illustrated in Table 4, Figure 5). The diminished density occurs in conjunction with increased glomerular volumes (0.530 ± 0.051 *versus* 0.270 ± 0.017 μm^3 BTBR *ob/ob versus* BTBR WT at 20 weeks; $P < 0.001$). There was no increase in the number of apoptotic podocytes in the

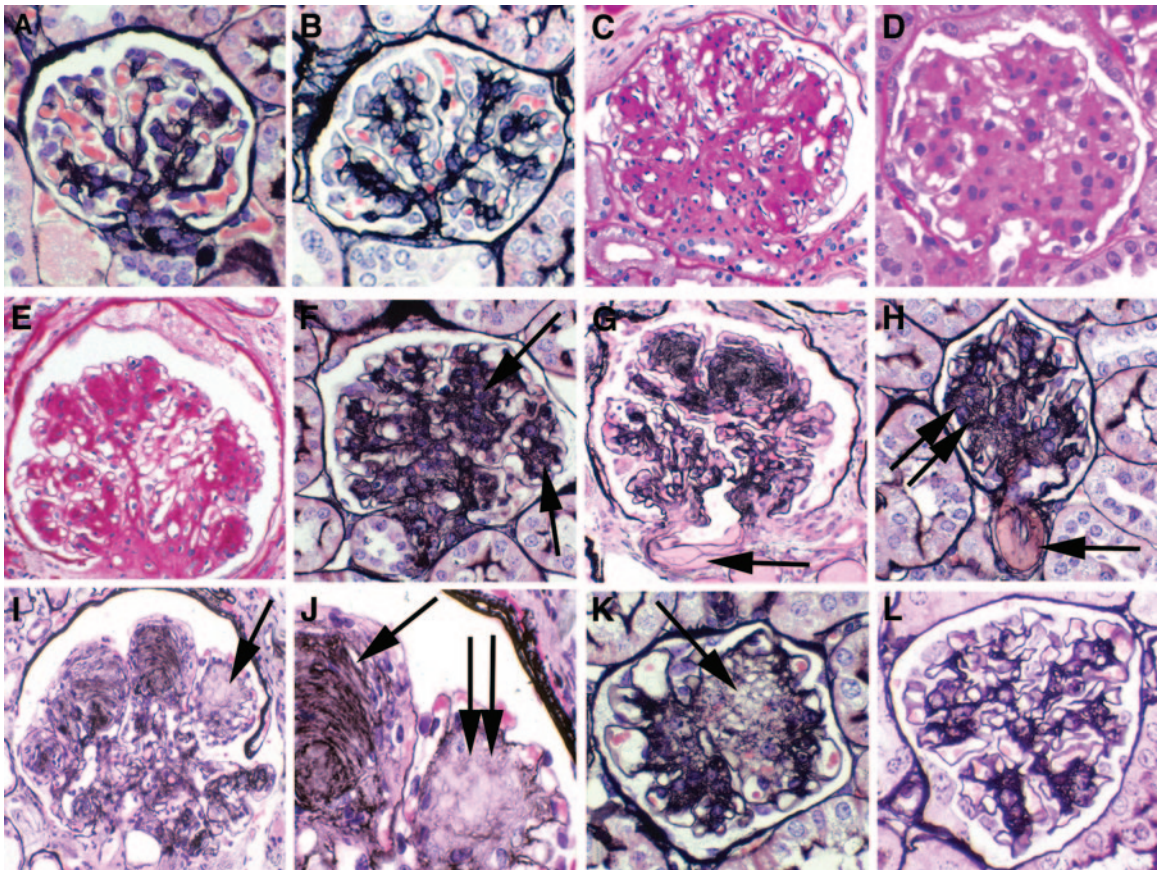

Figure 2. The BTBR *ob/ob* mouse models human DN. Advanced DN in the BTBR *ob/ob* mouse with comparisons to human DN and other murine models of DN. The BTBR *ob/ob* mouse is a good model of human DN, revealed by the histologic appearances of representative glomeruli from mice and humans with diabetes. (A and B) Normal-appearing glomeruli from a control BTBR mouse (A) and BTBR *ob/+* heterozygote mouse (B), both without diabetes. (C) Human DN demonstrating diffuse mesangial sclerosis. (D) Comparable appearance of BTBR *ob/ob* mouse at 20 weeks, showing diffuse mesangial sclerosis. (E) Human DN with nodular mesangial sclerosis. (F) Comparable appearance of BTBR *ob/ob* mouse at 20 weeks demonstrating progressive mesangial sclerosis approaching nodular mesangial sclerosis (arrows). (G) Human DN with characteristic hyalinosis of arterioles (arrow). (H) Comparable hyalinosis of arteriole in 21-week-old BTBR *ob/ob* mouse (arrow). The glomerulus shows diffuse and focally nodular (double arrow) mesangial sclerosis. (I) Human diabetic glomerulosclerosis with nodular mesangial sclerosis and focal lucency and dissolution of the normally compact mesangial matrix (arrow), indicative of mesangiolysis, compared with adjacent nodules composed of solidified matrix. (J) High-power view of H, demonstrating nodular glomerulosclerosis with laminated matrix indicative of repetitive episodes of mesangiolysis and repair (single arrow) and adjacent nodule undergoing mesangiolysis (double arrow). (K) Comparable focus of mesangiolysis with lucency and dissolution of the mesangial matrix in a 20-week-old BTBR *ob/ob* mouse (arrow). (L) Comparison of human DN in G, I, and J and comparable BTBR *ob/ob* changes in H and K with the limited mesangial change in similarly aged (22 weeks) leptin receptor–deficient *db/db* KS mice, the most widely used murine model of DN in type 2 diabetes, shown in L. A, B, and F through L, silver methenamine stain; C through E, periodic acid–Schiff stain.

BTBR *ob/ob* mice at either early (8 weeks) or late (20 weeks) time points compared with WT littermates, and only extremely rarely were any terminal deoxynucleotidyl transferase–mediated digoxigenin-deoxyuridine nick-end labeling (TUNEL)-positive podocytes seen in any of the tissue sections examined (data not shown).

Interstitial Fibrosis

Diffuse interstitial fibrosis was not detected using conventional histologic stains in any cohort studied, although focal and mild fibrosis was present in ≥12-week-old BTBR *ob/ob* mice (Supplemental Figure 2). Computer-aided morphometry performed on picrosirius red–stained slides to measure the degree of interstitial collagen accumulation showed significantly increased collagen accumulation in BTBR *ob/ob* mice at 24 weeks when compared with BTBR WT littermates (0.01000 ± 0.00180 *versus* $0.00086 \pm 0.00025\%$; $P < 0.001$, percentage of cortical interstitial area picrosirius red positive, excluding perivascular areas).

Comparisons with Controls

Comparisons of renal structural alterations achieved in BTBR and C57BL/6 mice treated with STZ (Supplemental Figure 6), C57BL/6 *ob/ob* mice (Figure 3E), and C57BLKS/J *db/db* (Figure 2L) with those in comparably aged BTBR *ob/ob* mice (Figure 2, D, F, and K) are illustrated in multiple

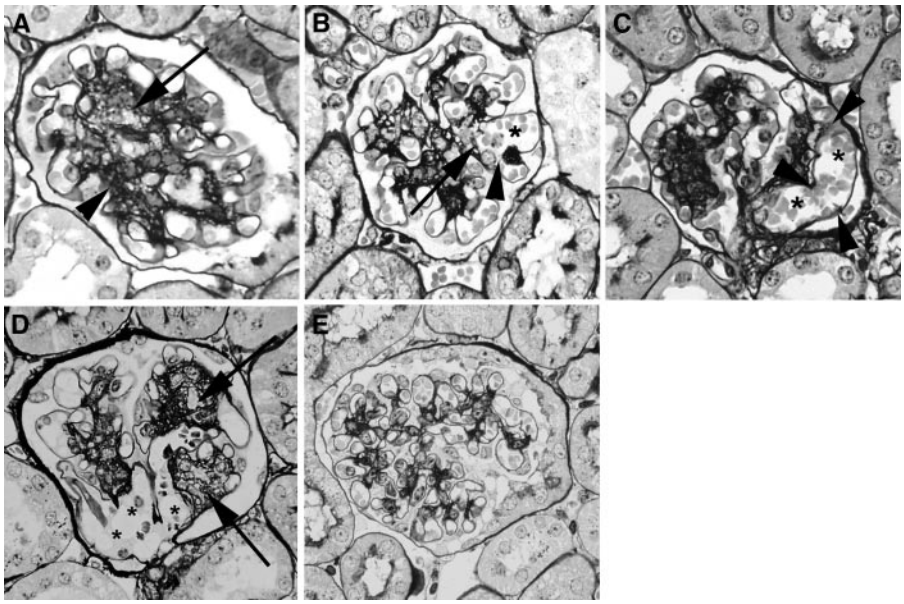

Figure 3. Mesangiolysis in BTBR *ob/ob* mice occurs at early and late stages in the evolution of DN. (A) Glomerulus from an 8-week-old BTBR *ob/ob* mouse shows characteristic, segmental dissolution (arrow) of normally compact silver staining matrix apparent in other mesangial regions (arrowhead). (B) Eight-week-old glomerulus demonstrates mesangiolysis (arrowhead) resulting in disrupted sites where capillary loops are anchored into the mesangium (arrow), leading to marked dilation/ballooning of the capillary loop (*). (C) A second example of mesangiolysis in 8-week-old BTBR *ob/ob* mice, with attenuation of mesangial matrix at the capillary luminal interface with resultant loss of anchoring sites of glomerular capillaries (arrowheads), leading to aneurysmal dilation of the capillary loop (*). (D) In older mice (22 weeks), glomeruli show pronounced areas of mesangial lucency (arrows) as well as marked dilation/ballooning of capillary loops (*). (E) C57BL/6 *ob/ob* mice do not have markedly expanded mesangial matrix or mesangiolysis.

figures. There was mildly to moderately increased mesangial matrix accumulation in STZ-treated BTBR WT mice at 38 weeks of age (30 weeks after STZ injection) compared with STZ-treated C57BL/6 mice and citrate buffer–treated control mice (BTBR WT and C57BL/6; Supplemental Figure 6). The generally mild and focally moderate mesangial matrix accumulation in STZ-treated mice was comparable to that in BTBR *ob/ob* mice at 8 weeks of age and exceeded that of 22-week-old C57BLKS *db/db* mice. The BTBR and C57BL/6 mice treated with STZ as well as the C57BL/6 *ob/ob* mice did not develop glomerular nodular lesions, arteriolar changes, or interstitial fibrosis. Supplemental Table 2 provides functional comparisons of blood glucose levels and albuminuria for these groups of mice. Together, these data demonstrate that hyperglycemia and BTBR strain or obesity are insufficient parameters for rapid development of the DN phenotype, but an interaction of BTBR strain and hyperglycemia with obesity and/or leptin deficiency also must be involved.

DISCUSSION

What are the key criteria for an animal model of DN? The National Institutes of Health–funded Animal Models of Diabetic Complications Consortium (AMDCC) recently revisited this question and proposed as guidelines the following three criteria for an ideal mouse model: (*1*) Progressive renal insufficiency in the setting of hyperglycemia, more specifically characterized as >50% decline in GFR during the lifetime of the animal; (*2*) albuminuria (>10-fold increase compared with age-, gender-, and strain-matched controls); and (*3*) characteristic pathologic changes including basement membrane thickening by electron microscopy, advanced mesangial matrix expansion with or without mesangiolysis and nodular mesangial sclerosis, interstitial fibrosis, and any degree of arteriolar hyalinosis.[5,7] It was explicitly recognized by the consortium that it may not be possible to achieve all of these alterations in models that nonetheless remain useful.

The BTBR *ob/ob* mouse model of DN comes close to meeting all of the proposed criteria of the AMDCC (albuminuria, pathologic changes) and offers several important advantages compared with existing DN models. The most important of these is the degree to which it reproduces essential structural and functional features of human diabetic glomerular injury. Glomerular hypertrophy, marked expansion of mesangial matrix, mesangiolysis, capillary basement membrane thickening, and loss of podocytes each have been identified as characteristic features of diabetic glomerular injury in humans, and each is present in the BTBR *ob/ob* model. The functional consequence of these changes in humans—marked proteinuria—also is present in this mouse model with a 10-fold increase in urinary protein excretion compared with controls.

Second, the model is robust and progressive: BTBR *ob/ob* mice uniformly develop features of DN and do so in a predictable time course in which podocyte loss is already detectable by 8 weeks of age and persists throughout the disease. The basis for podocyte loss was not established in this study, although the lack of significant apoptosis detected by TUNEL staining suggests other means of cell death or detachment are likely important. Studies are under way to investigate the mechanism of podocyte loss in these mice. Significant proteinuria is detectable as early as 8 weeks of age, corresponding with detectable podocyte loss, although it can be detected in some mice at even earlier ages, albeit without achieving statistical significance, when comparing 4-week-old cohorts with controls. Mesangiolysis is also an early feature of the disease, detectable in approximately 10% of glomeruli at 8 weeks of age, and coincides

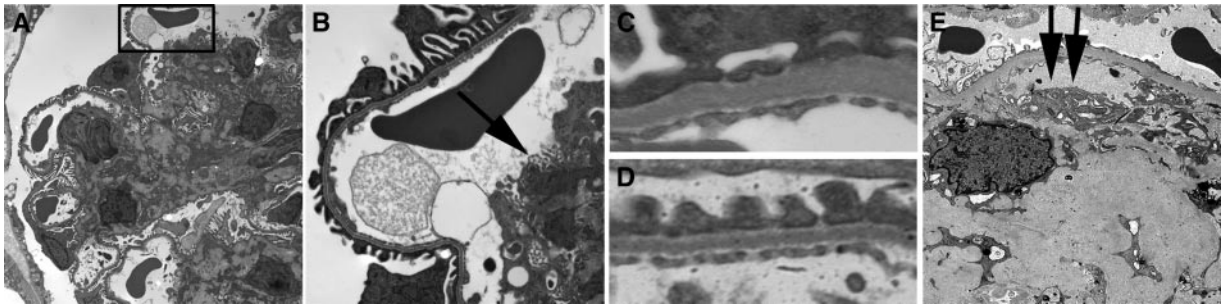

Figure 4. Ultrastructural changes in BTBR *ob/ob* mice resemble human DN. (A and B) Electron microscopy of glomeruli of 22-week-old BTBR *ob/ob* mice shows qualitatively good preservation of foot processes overall. There is increased mesangial matrix and evidence of mesangiolysis with fraying of the mesangial/capillary interface (arrows) in B. (C and D) Basement membranes are thickened and there is focal effacement of foot processes in BTBR *ob/ob* mice (C) when compared with BTBR WT mice (D). There is no evidence of immune deposits, confirmed by immunofluorescence studies (Supplemental Figure 4). (E) Advanced human DN, occurring after one or more decades of diabetes, also shows marked mesangial matrix accumulation, with similar fraying of the mesangial/capillary interface as seen in BTBR *ob/ob* mice (double arrows).

Table 2. BTBR *ob/ob* mice have significantly increased accumulations of mesangial matrix

Age (weeks)	Fractional Volume of Mesangial Matrix in Glomerular Tuft					
	BTBR WT	BTBR *ob/ob*	C57BL/6 WT	C57BL/6 *ob/ob*	C57BLKS/J *db/+*	C57BLKS/J *db/db*
8	13.20 ± 0.60	16.70 ± 0.90[a]	ND	ND	ND	ND
12	5.10 ± 1.90	13.10 ± 0.02[a]	ND	ND	ND	ND
16	11.70 ± 1.40	23.70 ± 1.40[b]	ND	ND	ND	ND
20	7.90 ± 1.60	18.30 ± 1.50[b]	ND	ND	ND	ND
22	6.70 ± 1.50	18.30 ± 1.50[a,c,d]	7.00 ± 0.16	6.95 ± 0.53	6.40 ± 2.50	7.80 ± 3.90
24	11.00 ± 2.20	19.70 ± 1.20[e,f]	ND	ND	4.90 ± 0.40	9.80 ± 2.70

The percentage of mesangial matrix within glomerular tuft area was determined by collagen IV–positive matrix in male BTBR WT, BTBR *ob/ob*, C57BL/6 WT, C5BL/6 *ob/ob*, C57BL/6 KS *db/+*, and C57BL/6 KS *db/db* mice at the time points shown ($n = 6$). Significant accumulation of mesangial matrix in BTBR *ob/ob* mice is seen as early as 8 weeks of age. ND, not done.
[a]$P < 0.01$ *versus* BTBR WT.
[b]$P < 0.001$ *versus* BTBR WT.
[c]$P < 0.01$ *versus* C57BL/6 *ob/ob*.
[d]$P < 0.05$ *versus* C57BLKS/J *db/db*.
[e]$P < 0.05$ *versus* BTBR WT.
[f]$P < 0.01$ *versus* C57BLKS/J *db/db*.

Table 3. BTBR *ob/ob* mice have significantly more Mac-2–positive cells per glomerulus compared with WT littermates starting at approximately 12 weeks of age, after the time point when mesangiolysis is seen in a number of glomeruli

Age (weeks)	Mac-2–Positive Monocyte/Macrophages per Glomerular Cross-Section (mean ± SEM)			
	Female		Male	
	BTBR WT	BTBR *ob/ob*	BTBR WT	BTBR *ob/ob*
4	0.62 ± 0.17	0.99 ± 0.21	0.74 ± 0.26	0.48 ± 0.08
8	0.77 ± 0.10	1.41 ± 0.17	0.68 ± 0.11	0.42 ± 0.03
12	ND	ND	0.89 ± 0.07	1.63 ± 0.24[a]
20	0.77 ± 0.11	1.40 ± 0.28	0.82 ± 0.19	2.20 ± 0.22[b]
22	0.75 ± 0.06	4.30 ± 0.79[a]	1.14 ± 0.17	10.5 ± 3.70[a]

[a]$P < 0.01$, [b]$P < 0.05$ *versus* age- and gender-matched WT littermates.

with detectable expansion of the mesangial matrix. These mesangial alterations are progressive. Many murine models of DN, such as STZ-induced DN, develop mild to moderate mesangial expansion and hence are good models of lesions occurring early in the course of human DN; the BTBR *ob/ob* mouse is among the very few models in which pronounced mesangial expansion and mesangiolysis, modeling advanced human DN, predictably develops.

Third, DN develops more rapidly in BTBR *ob/ob* mice compared with models of leptin receptor deficiency (*db/db* mice) or most other mouse models currently used to study DN,[7] which often require 30 to 50 weeks or more to develop relevant lesions. The relatively rapid onset allows opportunities for testing therapeutic strategies aimed at halting or ameliorating DN in a much shorter time span, especially important in the context of working with a model organism that under the best of circumstances has a lifespan of approximately 2 years.[11,18,19]

Fourth, there is increasing recognition of an inflammatory component in human and experimental DN, usually characterized by an influx of monocytes/macrophages. Progression of DN in the BTBR *ob/ob* mouse is also characterized by an influx of monocytes/macrophages. As in the hu-

Table 4. BTBR *ob/ob* mice have decreased podocyte number and podocyte density when compared to their WT littermates, apparent as early as 8 weeks of age, reaching statistical significance at 20 weeks of age

Parameter	BTBR WT	BTBR *ob/ob*
Podocyte no. (per glomerular tuft)		
8 weeks	85.44 ± 12.61	69.57 ± 6.50
20 weeks	96.28 ± 6.70	70.77 ± 6.41[a]
Glomerular volume ($\times 10^6$ μm^3)		
8 weeks	0.210 ± 0.014	0.290 ± 0.023
20 weeks	0.270 ± 0.017	0.530 ± 0.051[b,c]
Podocyte density (cell number/100 μm^3 glomerular volume)		
8 weeks	4.01 ± 0.46	2.49 ± 0.28[a]
20 weeks	3.57 ± 0.33	1.35 ± 0.10[b]
24 weeks	ND	1.20 ± 0.15[d]
28 weeks	ND	0.99 ± 0.13[d]

The BTBR *ob/ob* mice also have significantly increased glomerular volume ($n = 5$ to 7 per group). ND, not done.
[a] $P < 0.05$, [b] $P < 0.001$ *versus* age-matched BTBR WT littermates.
[c] $P < 0.001$ *versus* 8-week BTBR *ob/ob* and WT.
[d] $P < 0.001$ *versus* 20-week BTBR WT.

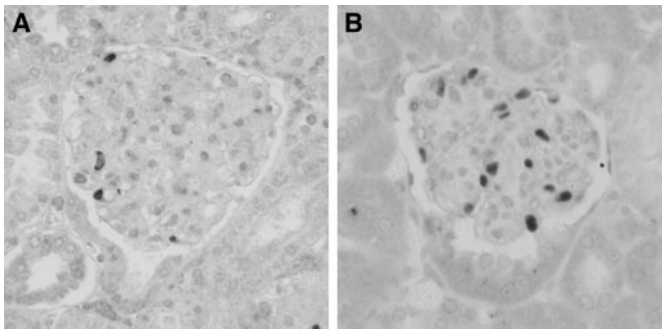

Figure 5. BTBR *ob/ob* mice have reduced podocyte number. (A and B) There is a reduction in podocyte number, assessed by WT-1 staining, in BTBR *ob/ob* (A) compared with BTBR WT (B) mice.

man lesions, it is not clear whether subpopulations of these cells change during the course of the disease and whether subsets of monocytes/macrophages mediate specific injury processes such as mesangiolysis or contribute to progressive injury, repair, or both. Finally, the absence of hypertension in this model allows identification of mediators of DN independent of the confounding effects of coexisting hypertension as may occur in other models.

The BTBR *ob/ob* model compares favorably with other leading murine models of advanced DN—those based on endothelial nitric oxide synthase deficiency ($eNOS^{-/-}$) in which diabetes is induced by STZ or by introducing the *db/db* mutation.[20,21] These models, unlike STZ-induced DN in other strains, have in common the features of mesangiolysis. We hypothesize, on the basis of this finding and the common finding of mesangiolysis in advanced human DN, that mesangiolysis is an essential injury for the development of advanced DN. Two key differences between the BTBR and $eNOS^{-/-}$ models are that the BTBR leptin-deficient model offers the potential of reversibility of established DN lesions with administration of leptin that is currently lacking in murine models in which eNOS is constitutively absent and that the BTBR model lacks the low level of confounding endothelial injury and tendency to thrombogenicity that has been reported in $eNOS^{-/-}$ mice.[20] It has been reported that mesangiolysis and mesangial nodular lesions can be prevented by insulin or antihypertensive therapy in $eNOS^{-/-}$ mice made diabetic by STZ.[22] The possibility that the unique susceptibility to DN in BTBR *ob/ob* mice may be due to endothelial dysfunction akin to the defects resulting from eNOS deficiency is being explored.

Like any animal model system, there also are limitations to the BTBR *ob/ob* model. Most important, this is a strain-dependent model system, as demonstrated by the striking differences between diabetic insulin-resistant BTBR *ob/ob* mice and similarly obese but nondiabetic C57BL/6 *ob/ob* mice. BTBR is not a strain familiar to many investigators; however, as differences in strain (and genetic background in humans) have become increasingly recognized as critical determinants of susceptibility to diabetes and nephropathy, this unique background may also be something of an advantage. It has been recognized that the most widely used mouse strain for chemical induction of diabetes by STZ, C57BL/6, is in fact poorly disposed to develop DN.[7] A series of genetic studies of BTBR *ob/ob* mice have identified the genes responsible for insulin resistance and further have identified networks of gene expression in pancreas, adipose tissue, liver, skeletal muscle, and brain that mediate various metabolic abnormalities consequent to diabetes.[23] These studies have the potential to provide a basis for understanding pathogenic events in the development of DN that may involve extrarenal sites and systemic perturbations consequent to diabetes and identify genetic differences between BTBR *ob/ob* mice and DN-resistant mice that may help elucidate critical mechanisms underlying DN. As an example, one gene identified by this analysis, *SORCS1*, has recently been identified as one of many genes where variants contribute to diabetes risk and glycemic control in humans, further demonstrating the utility of this model for understanding human disease.[19,24]

A second potential limitation is that this is a mouse model dependent on both strain (BTBR) and leptin deficiency. Overt leptin deficiency is not a characteristic of human diabetes, although the obesity commonly encountered in patients with type 2 diabetes is associated with leptin resistance.[25] This places limits on the overall similarity of leptin-deficient mouse models to the human condition. Nonetheless, the similarity of the diabetic complications that develop in this model to those in humans establish it as a valuable tool to investigate DN and other complications. A third important limitation is that al-

though the glomerular alterations strongly model those of human DN, the degree of interstitial fibrosis achieved at the time points studied, although measurably different from controls, is histologically modest overall. Concomitant measures of serum BUN and creatinine have also failed to suggest significant renal insufficiency. A likely basis for this lack of progressive renal insufficiency in this model despite marked glomerular changes is that measurable loss of renal function and interstitial fibrosis are processes occurring later in the disease course than the glomerulopathy. Although fibrotic changes are present at 20 to 22 weeks, this is an insufficient period for these changes to become advanced or for the most advanced changes of global glomerulosclerosis to develop. We may also detect loss of renal function when we are able to use the more sensitive direct measure of GFR rather than rely on a relatively insensitive measure of serum creatinine for this purpose.

Despite the susceptibility to diabetes and development of DN in BTBR *ob/ob* mice, studies by the group of Attie *et al.*[13] have shown that lean BTBR mice are normally insulin resistant (high circulating insulin levels) but normoglycemic. These mice are resistant to STZ-induced hyperglycemia, requiring much higher dosages to achieve similar blood glucose levels than STZ-treated C57BL/6 mice, a finding that was confirmed in this study. Hyperglycemic BTBR WT mice developed only modest manifestations of DN, after 30 weeks of hyperglycemia. The unique susceptibility of BTBR *ob/ob* mice toward developing diabetic complications requires both the BTBR genetic background and metabolic abnormalities conferred by the *ob/ob* mutation.

We anticipate the BTBR *ob/ob* mouse will prove an attractive model for study because unlike most other murine models of DN, not only do they develop lesions similar to human DN, but also there is preliminary evidence that complications in other organ systems that are typically encountered in humans with diabetes, such as cardiomyopathy[26] and liver disease (data not shown), develop in this model. As a model of leptin deficiency (unlike the *db/db* leptin receptor–deficient mouse), these mice offer the potential for reversal of disease with leptin administration. Preliminary studies by our laboratory indicate regression of nephropathy can be achieved by this approach; these studies will be the subject of a separate report.

CONCISE METHODS

Animals

The experimental protocol was reviewed and approved by the Animal Care Committee of the University of Washington in Seattle. The establishment of BTBR *ob/ob* mice has been previously described.[11,12] Breeding pairs of BTBR WT, BTBR/*ob* heterozygotes [BTBR$ob^{+/-}$; BTBR.V(B6)-Lep^{ob}/WiscJ; stock no. 004824]), C57BLKS/J $Lepr^{db}$ (C57BLKS/J *db/db*), and C57BL/6J/*ob* mice were purchased from Jackson Laboratories (Bar Harbor, ME) and maintained in an specific pathogen–free facility with a 12-hour light cycle and with free access to standard diet and water. Male and female BTBR *ob/ob,* BTBR WT, C57BLKS/J *db/db*, and C57BLKS/J *db/+* littermate mice were killed serially at 4, 8, 12, 16, 20, 22, and 24 weeks of age ($n = 6$ each group). A group of 28-week-old BTBR *ob/ob* mice ($n = 7$) were also studied. Male and female C57BL/6 *ob/ob* and WT littermate mice were killed at 22 and 24 weeks of age ($n = 6$).

As additional controls, male BTBR and C57BL/6 mice were made diabetic by five daily injections of STZ (80 and 50 mg/kg, respectively) beginning at 8 weeks of age and killed at 38 weeks of age ($n = 8$ BTBR) and 45 weeks of age ($n = 8$ C57BL/6), after 30 and 37 weeks of hyperglycemia, respectively. Control mice received five daily injections of citrate. The higher dosage of STZ used in BTBR mice was established in pilot studies conducted to determine the optimal dosage of STZ required to induce diabetes. BTBR WT mice received five daily STZ injections of 40, 50, 60, or 80 mg/kg ($n = 3$). The mice had an average starting blood glucose level of 130.3 $\pm$ 4.2 mg/dl, and this was not appreciably increased by the 40, 50, or 60 mg/kg STZ injections (average blood glucose levels of 100.7 $\pm$ 45.7, 130.7 $\pm$ 18.8, and 156.0 $\pm$ 3.8 mg/dl, respectively), whereas the 80-mg/kg dose resulted in an average blood glucose level of 287.7 $\pm$ 43.9 mg/dl after 3 weeks. C57 BL/6 mice treated with five daily doses of STZ at 50 mg/kg achieved blood glucose levels of 342.3 $\pm$ 22.3 mg/dl in the same pilot study.

Blood Chemistry

Blood samples were obtained by saphenous vein puncture and at the time when mice were killed. Blood glucose levels were monitored using a Freestyle Blood Glucose Monitor (Abbott Diabetes Care, Alameda, CA).

BUN was measured using the QuantiChrom Urea Assay Kit (BioAssay Systems, Hayward CA). Serum creatinine levels were measured by an HPLC-based method at the Yale University Mouse Metabolic Phenotyping Center metabolic testing core.

Urine Measurements

Timed (12 hour) urine and spot urine samples were collected from individual mice before being killed. Urine was collected during the evening dark cycle, with the mice having access to water but not food. Urinary albumin was measured using the Albuwell M Murine ELISA kit (Exocell, Philadelphia PA), and urinary creatinine was measured with the Creatinine Companion kit (Exocell). Total albumin measured in 12-hour samples was multiplied by 2 to obtain a 24-hour protein excretion rate.

BP Measurement

BPs were measured using the Coda-6 VPR tail-cuff system (Kent Scientific, Torrington, CT)[27,28] on conscious mice, as described previously,[29] before mice were killed at the time points described already ($n = 6$ each group).

Histologic Analysis

Kidneys and other organs were obtained from BTBR WT, BTBR *ob/ob*, C57BL/6 *ob/ob,* C57BL/6 WT, C57BLKS/J *db/db*, C57BLKS/J *db/+*, and STZ-treated BTBR and C57BL/6 mice at each of the previously indicated time points, and portions were immersion-fixed in 10% neutral-buffered formalin and in methyl Carnoy fixative. Tissues were embedded in paraffin using standard methods; sectioned; and stained with silver methenamine, periodic acid–Schiff, hematoxylin and eosin, and picrosirius red reagents. Selected tissues fixed in ½ strength Karnovsky solution were processed, sectioned, and examined by electron

microscopy according to standard protocols. In cases examined by this technique, a series of 10 photographs were taken at ×12,000 magnification, a grid was overlaid on the photograph and basement membrane thickness was measured at points where it intersected with the grid.

Immunohistochemistry and TUNEL

Four-micrometer sections of formalin or methyl Carnoy–fixed, paraffin-embedded tissue were immunostained as described previously.[30,31] The antibodies used were (*1*) rat anti–Mac-2 (Cedarlane; Hornby, Ontario, Canada[32]) to detect infiltrating monocytes/macrophages; (*2*) mouse anti–α-SMA, clone 1A4 (Sigma, St. Louis, MO); (*3*) rabbit anti–WT-1 (Santa Cruz Biotechnology, Santa Cruz, CA) to mark podocyte nuclei; (*4*) rat anti–Ki-67, clone Tec3 (Dako, Carpinteria, CA), as a measure of cell proliferation; and (*5*) rabbit anti–collagen IV (Southern Biotechnology, Birmingham, AL). Negative controls for immunohistochemistry included both substitution of the primary antibody with an isotype-matched irrelevant Ig or antisera from the same species and substitution with PBS. Immunofluorescence was performed on frozen tissue sections to detect the presence of IgG, IgA, IgM, and C3 as described previously.[33] Apoptotic cells were detected using the ApopTag Plus kit (Chemicon Int., Temecula, CA) according to the manufacturer's instructions.

Quantitative Analysis of Glomerular and Interstitial Lesions

For each animal, 20 0.1-mm^2 section areas were randomly photographed under ×400 magnification, and the glomerular cross-sectional area and degree of glomerular matrix accumulation (collagen IV expression and silver methenamine stain), mesangial actin expression, and area occupied by α-SMA–positive activated mesangial cells were quantified by computer image analysis (ImagePro Plus image analysis software) as described previously.[30,34] Mac-2–positive monocyte/macrophages within glomeruli were counted in a minimum of 50 glomerular cross-sections and expressed as average number of cells per glomerular area. Silver methenamine–stained histologic sections were examined in a blinded manner, and the number of glomeruli exhibiting mesangiolysis (defined as dissolution with areas of lucency of mesangial regions that normally exhibit compact silver staining matrix and/or marked microaneurysmal dilation of adjacent glomerular capillaries) in an entire cross-sectional kidney section was counted. Slides stained with picrosirius red were photographed under polarized light to achieve maximal brightness, and the percentage of positive interstitial staining was quantified using ImagePro Plus software.

Enumeration of Podocytes

Podocyte counting was performed on 3-μm sections of formalin-fixed tissue immunostained with a marker of podocyte nuclei (WT-1). Fifty stained glomerular sections were digitally photographed, and the images were imported into the ImagePro Plus software and analyzed morphometrically. The estimation of the average number of podocytes per glomerulus is then determined by the stereologic method published by Weibel,[35] which is based on determining density of podocytes (identified by their WT-1 expression in nuclei) per glomerulus in histologic slides, and the multiplication of this density by the measured glomerular volume to obtain podocyte cell number, as used by others.[36–38]

Because of published concerns by others that this method may overestimate absolute podocyte numbers,[39] a second approach to measure podocyte number and podocyte density was also used. We followed the method of Sanden *et al.*[40] by using WT-1–stained nuclei to enumerate podocytes in kidney tissue sections of uneven thickness (3 and 9 μm). After glomerular volumes were calculated, the counted podocyte nuclei were used to determine podocyte density, a measure that overcomes the problem of cell counts in glomeruli of unequal sizes and that may be a better measure of podocyte integrity.[7,41]

Statistical Analysis

All values are expressed as the mean ± SEM. Analysis was performed using InStat StatView for Windows (GraphPad Software, La Jolla, CA), using one-way ANOVA and the Tukey-Kramer Multiple Comparisons Test or the unpaired two-tailed *t* test to determine *P* values.

ACKNOWLEDGMENTS

This work was supported by an National Institute of Diabetes and Digestive and Kidney Diseases Mouse Metabolic Phenotypic Center's MICROMouse funding program (grant DK076169) and by National Institutes of Health grant DK076126 to the Seattle Mouse Metabolic Phenotyping Center, and by National Institutes of Health grants DK66369 and DK58037 to A.D.A. Measurement of creatinine by HPLC was performed by the Yale MMPC Analytic Core facility, supported in part by National Institute of Diabetes and Digestive and Kidney Diseases grant U24DK76169.

Portions of this work were presented at the annual meetings of the American Society of Nephrology, November 14 through 19, 2006, San Diego, CA; and November 5 through 9, 2008, Philadelphia, PA.

DISCLOSURES

None.

REFERENCES

1. US Renal Data System: *USRDS 2004 Annual Data Report*, Bethesda, National Institutes of Health, National Institute of Diabetes and Digestive and Kidney Diseases, 2004
2. National Kidney Foundation: K/DOQI clinical practice guidelines for chronic kidney disease: Evaluation, classification, and stratification. *Am J Kidney Dis* 39[Suppl 1]: S1–S266, 2002
3. Mohanram A, Toto RD: Outcome studies in diabetic nephropathy. *Semin Nephrol* 23: 255–271, 2003
4. Narayan KM, Boyle JP, Thompson TJ, Sorensen SW, Williamson DF: Lifetime risk for diabetes mellitus in the United States. *JAMA* 290: 1884–1890, 2003
5. Breyer MD, Bottinger E, Brosius FC, Coffman TM, Fogo A, Harris RC, Heilig CW, Sharma K: Diabetic nephropathy: Of mice and men. *Adv Chronic Kidney Dis* 12: 128–145, 2005
6. Breyer MD, Bottinger E, Brosius FC 3rd, Coffman TM, Harris RC, Heilig CW, Sharma K: Mouse models of diabetic nephropathy. *J Am Soc Nephrol* 16: 27–45, 2005
7. Brosius FC 3rd, Alpers CE, Bottinger EP, Breyer MD, Coffman TM, Gurley SB, Harris RC, Kakoki M, Kretzler M, Leiter EH, Levi M, McIndoe RA,

Sharma K, Smithies O, Susztak K, Takahashi N, Takahashi T: Mouse models of diabetic nephropathy. *J Am Soc Nephrol* 20: 2503–2512, 2009
8. Janssen U, Phillips AO, Floege J: Rodent models of nephropathy associated with type II diabetes. *J Nephrol* 12: 159–172, 1999
9. Tesch GH, Nikolic-Paterson DJ: Recent insights into experimental mouse models of diabetic nephropathy. *Nephron Exp Nephrol* 104: e57–e62, 2006
10. Jefferson JA, Shankland SJ, Pichler RH: Proteinuria in diabetic kidney disease: A mechanistic viewpoint. *Kidney Int* 74: 22–36, 2008
11. Clee SM, Nadler ST, Attie AD: Genetic and genomic studies of the BTBR ob/ob mouse model of type 2 diabetes. *Am J Ther* 12: 491–498, 2005
12. Ranheim T, Dumke C, Schueler KL, Cartee GD, Attie AD: Interaction between BTBR and C57BL/6J genomes produces an insulin resistance syndrome in (BTBR x C57BL/6J) F1 mice. *Arterioscler Thromb Vasc Biol* 17: 3286–3293, 1997
13. Clee SM, Attie AD: The genetic landscape of type 2 diabetes in mice. *Endocr Rev* 28: 48–83, 2007
14. Stoehr JP, Byers JE, Clee SM, Lan H, Boronenkov IV, Schueler KL, Yandell BS, Attie AD: Identification of major quantitative trait loci controlling body weight variation in ob/ob mice. *Diabetes* 53: 245–249, 2004
15. Stoehr JP, Nadler ST, Schueler KL, Rabaglia ME, Yandell BS, Metz SA, Attie AD: Genetic obesity unmasks nonlinear interactions between murine type 2 diabetes susceptibility loci. *Diabetes* 49: 1946–1954, 2000
16. Aizawa-Abe M, Ogawa Y, Masuzaki H, Ebihara K, Satoh N, Iwai H, Matsuoka N, Hayashi T, Hosoda K, Inoue G, Yoshimasa Y, Nakao K: Pathophysiological role of leptin in obesity-related hypertension. *J Clin Invest* 105: 1243–1252, 2000
17. Burgueno AL, Landa MS, Schuman ML, Alvarez AL, Carabelli J, Garcia SI, Pirola CJ: Association between diencephalic thyroliberin and arterial blood pressure in agouti-yellow and ob/ob mice may be mediated by leptin. *Metabolism* 56: 1439–1443, 2007
18. Clee SM, Yandell BS, Schueler KM, Rabaglia ME, Richards OC, Raines SM, Kabara EA, Klass DM, Mui ET, Stapleton DS, Gray-Keller MP, Young MB, Stoehr JP, Lan H, Boronenkov I, Raess PW, Flowers MT, Attie AD: Positional cloning of Sorcs1, a type 2 diabetes quantitative trait locus. *Nat Genet* 38: 688–693, 2006
19. Goodarzi MO, Lehman DM, Taylor KD, Guo X, Cui J, Quinones MJ, Clee SM, Yandell BS, Blangero J, Hsueh WA, Attie AD, Stern MP, Rotter JI: SORCS1: A novel human type 2 diabetes susceptibility gene suggested by the mouse. *Diabetes* 56: 1922–1929, 2007
20. Nakagawa T, Sato W, Glushakova O, Heinig M, Clarke T, Campbell-Thompson M, Yuzawa Y, Atkinson MA, Johnson RJ, Croker B: Diabetic endothelial nitric oxide synthase knockout mice develop advanced diabetic nephropathy. *J Am Soc Nephrol* 18: 539–550, 2007
21. Zhao HJ, Wang S, Cheng H, Zhang MZ, Takahashi T, Fogo AB, Breyer MD, Harris RC: Endothelial nitric oxide synthase deficiency produces accelerated nephropathy in diabetic mice. *J Am Soc Nephrol* 17: 2664–2669, 2006
22. Kosugi T, Heinig M, Nakayama T, Connor T, Yuzawa Y, Li Q, Hauswirth WW, Grant MB, Croker BP, Campbell-Thompson M, Zhang L, Atkinson MA, Segal MS, Nakagawa T: Lowering blood pressure blocks mesangiolysis and mesangial nodules, but not tubulointerstitial injury, in diabetic eNOS knockout mice. *Am J Pathol* 174: 1221–1229, 2009
23. Keller MP, Choi Y, Wang P, Davis DB, Rabaglia ME, Oler AT, Stapleton DS, Argmann C, Schueler KL, Edwards S, Steinberg HA, Chaibub Neto E, Kleinhanz R, Turner S, Hellerstein MK, Schadt EE, Yandell BS, Kendziorski C, Attie AD: A gene expression network model of type 2 diabetes links cell cycle regulation in islets with diabetes susceptibility. *Genome Res* 18: 706–716, 2008
24. Paterson AD, Waggott D, Boright AP, Hosseini SM, Shen E, Sylvestre MP, Wong I, Bharaj B, Cleary PA, Lachin JM, Below JE, Nicolae D, Cox NJ, Canty AJ, Sun L, Bull SB: A genome-wide association study identifies a novel major locus for glycemic control in type 1 diabetes, as measured by both HbA1c and glucose. *Diabetes* 59: 539–549, 2010
25. Enriori PJ, Evans AE, Sinnayah P, Cowley MA: Leptin resistance and obesity. *Obesity (Silver Spring)* 14[Suppl 5]: 254S–258S, 2006
26. O'Brien K, Kim J, Wietecha T, Hudkins K, McDonald T, Minami E, Alpers C: A new murine model of diabetic cardiomyopathy: The female leptin-deficient, black and tan brachyuric mouse. *Circulation* 120: S490, 2009
27. Whitesall SE, Hoff JB, Vollmer AP, D'Alecy LG: Comparison of simultaneous measurement of mouse systolic arterial blood pressure by radiotelemetry and tail-cuff methods. *Am J Physiol Heart Circ Physiol* 286: H2408–H2415, 2004
28. Feng M, Whitesall S, Zhang Y, Beibel M, D'Alecy L, DiPetrillo K: Validation of volume-pressure recording tail-cuff blood pressure measurements. *Am J Hypertens* 21: 1288–1291, 2008
29. Guo S, Kowalewska J, Wietecha TA, Iyoda M, Wang L, Yi K, Spencer M, Banas M, Alexandrescu S, Hudkins KL, Alpers CE: Renin-angiotensin system blockade is renoprotective in immune complex-mediated glomerulonephritis. *J Am Soc Nephrol* 19: 1168–1176, 2008
30. Taneda S, Hudkins KL, Cui Y, Farr AG, Alpers CE, Segerer S: Growth factor expression in a murine model of cryoglobulinemia. *Kidney Int* 63: 576–590, 2003
31. Alpers CE, Seifert RA, Hudkins KL, Johnson RJ, Bowen-Pope DF: Developmental patterns of PDGF B-chain, PDGF-receptor, and alpha-actin expression in human glomerulogenesis. *Kidney Int* 42: 390–399, 1992
32. Rosenberg I, Cherayil BJ, Isselbacher KJ, Pillai S: Mac-2-binding glycoproteins: Putative ligands for a cytosolic beta-galactoside lectin. *J Biol Chem* 266: 18731–18736, 1991
33. Taneda S, Segerer S, Hudkins KL, Cui Y, Wen M, Segerer M, Wener MH, Khairallah CG, Farr AG, Alpers CE: Cryoglobulinemic glomerulonephritis in thymic stromal lymphopoietin transgenic mice. *Am J Pathol* 159: 2355–2369, 2001
34. Taneda S, Pippin JW, Sage EH, Hudkins KL, Takeuchi Y, Couser WG, Alpers CE: Amelioration of diabetic nephropathy in SPARC-null mice. *J Am Soc Nephrol* 14: 968–980, 2003
35. Weibel ER: *Practical Methods for Biological Morphometry*, London, Academic Press, 1979, pp 40–116
36. Pagtalunan ME, Miller PL, Jumping-Eagle S, Nelson RG, Myers BD, Rennke HG, Coplon NS, Sun L, Meyer TW: Podocyte loss and progressive glomerular injury in type II diabetes. *J Clin Invest* 99: 342–348, 1997
37. Steffes MW, Schmidt D, McCrery R, Basgen JM: Glomerular cell number in normal subjects and in type 1 diabetic patients. *Kidney Int* 59: 2104–2113, 2001
38. Macconi D, Bonomelli M, Benigni A, Plati T, Sangalli F, Longaretti L, Conti S, Kawachi H, Hill P, Remuzzi G, Remuzzi A: Pathophysiologic implications of reduced podocyte number in a rat model of progressive glomerular injury. *Am J Pathol* 168: 42–54, 2006
39. White KE, Bilous RW: Estimation of podocyte number: A comparison of methods. *Kidney Int* 66: 663–667, 2004
40. Sanden SK, Wiggins JE, Goyal M, Riggs LK, Wiggins RC: Evaluation of a thick and thin section method for estimation of podocyte number, glomerular volume, and glomerular volume per podocyte in rat kidney with Wilms' tumor-1 protein used as a podocyte nuclear marker. *J Am Soc Nephrol* 14: 2484–2493, 2003
41. Siu B, Saha J, Smoyer WE, Sullivan KA, Brosius, FC 3rd: Reduction in podocyte density as a pathologic feature in early diabetic nephropathy in rodents: Prevention by lipoic acid treatment. *BMC Nephrol* 7: 6, 2006

See related editorial, "Progress in Progression?" on pages 1414–1416.

Supplemental information for this article is available online at http://www.jasn.org/.